Diffusion-driven front instabilities in the chlorite–tetrathionate reaction

Dezső Horváth and Ágota Tóth

Citation: The Journal of Chemical Physics **108**, 1447 (1998); doi: 10.1063/1.475355
View online: http://dx.doi.org/10.1063/1.475355
View Table of Contents: http://scitation.aip.org/content/aip/journal/jcp/108/4?ver=pdfcov
Published by the AIP Publishing

Diffusion-driven front instabilities in the chlorite–tetrathionate reaction

Dezső Horváth and Ágota Tóth
Department of Physical Chemistry, József Attila University, P.O. Box 105, Szeged, H-6701 Hungary

(Received 4 June 1997; accepted 15 October 1997)

An extensive study on the instabilities of planar fronts leading to the formation of cellular structures has been carried out in the acid-catalyzed chlorite–tetrathionate reaction. A simple two-variable model based on the empirical rate law of the reaction is developed to describe the observed pattern formation. The calculated onset of instability and the size of the patterns in the cellular fronts are in good agreement with experimental observations. © *1998 American Institute of Physics.* [S0021-9606(98)50904-X]

I. INTRODUCTION

Pattern formation in reaction–diffusion systems as a result of instabilities in the homogeneous states has been the focus of numerous theoretical[1–5] and experimental[6–11] investigations. In the classical example of Turing structures,[1,6–8] the concentration distribution of some intermediate species in a two-dimensional space can be characterized by the formation of stationary spots and stripes. The interaction of steady states in a bistable system may also lead to the appearance of replicating spots and serpentine patterns in an open spatial medium.[9–11] In closed systems, transient patterns arise in the form of cellular fronts between homogeneous states of the reactants and products.[12–16] Besides special kinetics such as autocatalysis and inhibition, the essential in all of these cases is the spatial decoupling of the key species so that the activator—the component with autocatalytic characteristics—has lower diffusivity than the inhibitor. In experimental studies, the selective lowering of the effective diffusion coefficient is achieved by binding the autocatalyst into an immobile species. Starch is used for binding triiodide in Turing structures of the chlorite–iodide–malonic acid reaction,[6,7,17] α-cyclodextrin for binding iodide in fronts of the iodate–arsenous acid reaction,[15] and immobile carboxylate ions for binding hydrogen ions in fronts of the chlorite–tetrathionate reaction.[16] The underlying reaction kinetics is generally complex, exhibiting bistability and oscillations in homogeneous systems, although instabilities of planar fronts leading to cellular structures may appear in simple autocatalytic reactions where the order with respect to the autocatalyst is higher than unity in the rate law.[14] These patterned fronts of simple autocatalytic reactions share common features with cellular premixed flames,[18,19] where the role of temperature via the Arrhenius kinetics is equivalent to that of the autocatalyst in the autocatalytic reactions under isothermal conditions.

In this work a systematic study of the recently discovered cellular fronts of the chlorite oxidation of tetrathionate ion[16] is carried out. The reaction

$$7\mathrm{ClO_2^-}+2\mathrm{S_4O_6^{2-}}+6\mathrm{H_2O}\rightarrow 7\mathrm{Cl^-}+8\mathrm{SO_4^{2-}}+12\mathrm{H^+}, \quad \text{(R1)}$$

run in slight chlorite excess, is acid-catalyzed and satisfies the kinetic requirement for front instability, as in the determined empirical rate law,

$$r=-\frac{1}{7}\frac{d[\mathrm{ClO_2^-}]}{dt}=k[\mathrm{ClO_2^-}][\mathrm{S_4O_6^{2-}}][\mathrm{H^+}]^2, \quad (1)$$

the autocatalyst hydrogen ion has an order of two.[20] The partial immobilization of hydrogen ions is obtained by incorporating carboxylate groups in the form of methacrylate in the hydrogel polymer used for ensuring a convection-free environment, which reversibly binds the autocatalyst via a fast equilibrium,

$$\mathrm{H^+}+-\mathrm{COO^-}\rightleftharpoons -\mathrm{COOH}, \quad \text{(R2)}$$

without interfering with the main reaction. The critical methacrylate concentration representing the onset of instability for planar fronts has been determined by varying the amount of carboxylate groups in the hydrogel and measuring the amplitude of the developed fronts. The experimental conditions are presented in detail in Sec. II. A simple two-variable model based on the empirical rate law [Eq. (1)] quantitatively describes reaction–diffusion fronts of the reaction in slight chlorite excess.[21] This model is extended to include the equilibrium without the use of adjustable parameters in Sec. III. Finally, the results of calculations are compared with the experimental observations.

II. EXPERIMENTAL STUDY

Throughout the experiments, reagent-grade chemicals (Aldrich, Reanal) were used without further purification except sodium chlorite, which was recrystallized twice in ethanol–water mixture.[21]

To ensure a convection-free environment, the reactions were carried out in a polymer gel at room temperature ($23\pm2\,^\circ\mathrm{C}$). The thin polyacrylamide hydrogel with varying sodium methacrylate content ($c_M=0-0.021$ M corresponding to 0%–70% binding of the autocatalyst hydrogen ions) was prepared so that the total concentration of monomers was held constant at 2.76 M. Appropriate amounts of acrylamide, sodium methacrylate, and 0.2 g N,N'-methylenebisacrylamide were dissolved in 15 $\mathrm{cm^3}$ hot water. The solution was cooled down to 5 °C and 0.3 $\mathrm{cm^3}$ 30 V% triethanolamine was added. After 15 min of degassing, the polymerization was initiated by adding 30 mg $\mathrm{K_2S_2O_8}$ and the solution was injected into a mold sized 13 cm×9 cm×1 mm. The

TABLE I. Reagent concentrations in the solution.

$[K_2S_4O_6]$/M	0.005
$[NaClO_2]$/M	0.02
[NaOH]/M	0.0007
$[CH_3COONa]$/M	0.0015–0.0225
[Congo red]/(g cm^{-3})	0.0004

polymerization took place within 30 min, and finally the gel was rinsed thoroughly with doubly distilled water.

The prepared hydrogel was soaked in 100 cm^3 of reactant solution, with the composition given in Table I, for 15 min. A small amount of sodium hydroxide was included in the reactant mixture to eliminate self-initiation, and sodium acetate to ensure a constant pH-drop in the obtained fronts. Planar initiations were achieved by cutting the gel in two and rinsing the smaller part in dilute sulfuric acid, which resulted in the conversion of the reactant mixture into acidic product mixture. Having wiped off drops of solutions from the surface of the gels, the two parts were carefully attached, placed between two glass plates, and sealed to prevent evaporation around the edges.

The propagation of fronts was monitored with a monochrome CCD camera (Panasonic WV-BP310/G) using diffuse light from a halogen lamp (150 W) as a light source and a broadband filter ($\lambda = 509$ nm, $\Delta\lambda = 91$ nm). Complete frames of 664×512 pixel were stored digitally by a computer-controlled frame grabber (AVER Pro 2000) in 300-3600 s intervals and further processed using standard procedures.

III. MODELING STUDY

Propagating reaction–diffusion fronts in the chlorite–tetrathionate acid-catalyzed reaction run in slight excess of chlorite can be described by a simple two-variable model based on the empirical rate law given in Eq. (1).[21]

In our system, hydrogen ions are partially bound to carboxylate groups of the immobile polymer chain via the fast equilibrium given in Eq. (R2) so that

$$[H^+] = \frac{K_d[-COOH]}{[-COO^-]} \tag{2}$$

is valid with K_d being the dissociation constant of the carboxylic acid groups. By considering Eq. (2), we can write down the governing equations of the system as

$$\frac{\partial[ClO_2^-]}{\partial t} = D_{ClO_2^-}\nabla^2[ClO_2^-] - 7r, \tag{3a}$$

$$\frac{\partial[S_4O_6^{2-}]}{\partial t} = D_{S_4O_6^{2-}}\nabla^2[S_4O_6^{2-}] - 2r, \tag{3b}$$

$$\frac{\partial[H^+]_t}{\partial t} = D_{H^+}\nabla^2[H^+] + 12r, \tag{3c}$$

where D_is are the appropriate diffusion coefficients and $[H^+]_t$ is the total concentration of the autocatalyst hydrogen ions given as

$$[H^+]_t = [H^+] + [-COOH]. \tag{4}$$

The diffusion coefficients of the reactant ions in aqueous solution are of the same magnitude; therefore, we can set $D \equiv D_{ClO_2^-} = D_{S_4O_6^{2-}}$ and hence eliminate Eq. (3a) by expressing the concentration of chlorite in terms of that of tetrathionate according to

$$[ClO_2^-] = \frac{2[ClO_2^-]_0 - 7[S_4O_6^{2-}]_0 + 7[S_4O_6^{2-}]}{2}, \tag{5}$$

where $[ClO_2^-]_0$ and $[S_4O_6^{2-}]_0$ are the appropriate initial concentrations far ahead of the front.

Considering Eq. (2) and the mass balance for methacrylate $c_M = [-COOH] + [-COO^-]$, the concentration of carboxylic acid groups can be given as a function of the free hydrogen ions:

$$[-COOH] = \frac{c_M[H^+]}{K_d + [H^+]}. \tag{6}$$

Applying Eqs. (4) and (6), the left-hand side of Eq. (3c) can now be expanded as

$$\frac{\partial[H^+]_t}{\partial t} = \frac{\partial[H^+]}{\partial t}\left(1 + \frac{c_M K_d}{(K_d + [H^+])^2}\right). \tag{7}$$

The substitution of Eqs. (5) and (7) back to Eq. (3) with the introduction of dimensionless variables $\alpha = [S_4O_6^{2-}]/[S_4O_6^{2-}]_0$ and $\beta = [H^+]/[S_4O_6^{2-}]_0$ leads to

$$\frac{\partial\alpha}{\partial\tau} = \tilde{\nabla}^2\alpha - \alpha\beta^2(\kappa + 7\alpha), \tag{8a}$$

$$\frac{\partial\beta}{\partial\tau} = \frac{\delta\tilde{\nabla}^2\beta}{\sigma} + \frac{6\alpha\beta^2(\kappa + 7\alpha)}{\sigma}, \tag{8b}$$

where $\delta = D_{H^+}/D$ is the ratio of the diffusion coefficients, $\kappa = 2[ClO_2^-]_0/[S_4O_6^{2-}]_0 - 7$ is the relative chlorite excess; $\tau = k[S_4O_6^{2-}]_0^3 t$ and $\tilde{\nabla}^2 \equiv \partial^2/\partial\xi^2 + \partial^2/\partial\eta^2 = D/(k[S_4O_6^{2-}]_0^3)\nabla^2$ represent dimensionless time and length scales. The coefficient $\sigma = 1 + (K\mu)/(K + \beta)^2$ with dimensionless parameter $K = K_d/[S_4O_6^{2-}]_0$ incorporates the methacrylate content of the gel via $\mu = c_M/[S_4O_6^{2-}]_0$, and accounts for the decrease in the effective diffusion coefficient for the autocatalyst hydrogen ion on increasing the concentration of methacrylate in the hydrogel.

The partial differential equations in Eq. (8) were solved numerically using an explicit Euler method with a standard nine-point formula to approximate the Laplacian. The calculations were carried out on a two-dimensional grid of 201×401 points with no-flux boundary conditions. A grid spacing of $h = 0.4$ and a time step of $\Delta\tau = 10^{-3}$ were chosen for the integration so that the obtained concentration profiles were independent of them. The initial conditions reflected the experimental setup: at $\tau = 0$ the grid was divided into two areas, one corresponding to the reactant mixture with $\alpha = 1.0$, $\beta = 0.0$, and the other to the products with $\alpha = 0.0$, $\beta = 6.0 - \mu$. The inherent experimental noise was implemented in the initial concentration field by randomly shifting the lines of the grid one point in the direction of propagation. The param-

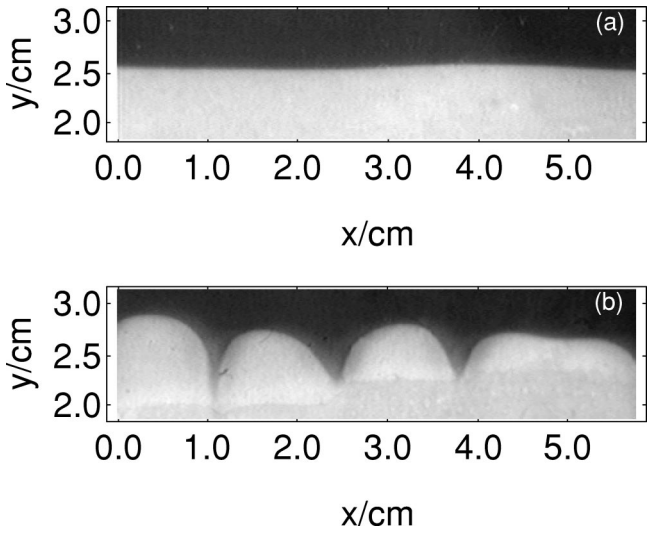

FIG. 1. Images of fronts developed from planar initiation for (a) $c_M = 6.0$ mM (20% binding of the autocatalyst) at $t = 2$ h; (b) $c_M = 21.0$ mM (70% binding) at $t = 12$ h. Darker regions represent the unreacted reactant mixture ahead of, and lighter ones the product mixture behind the front. The reactant concentrations are given in Table I.

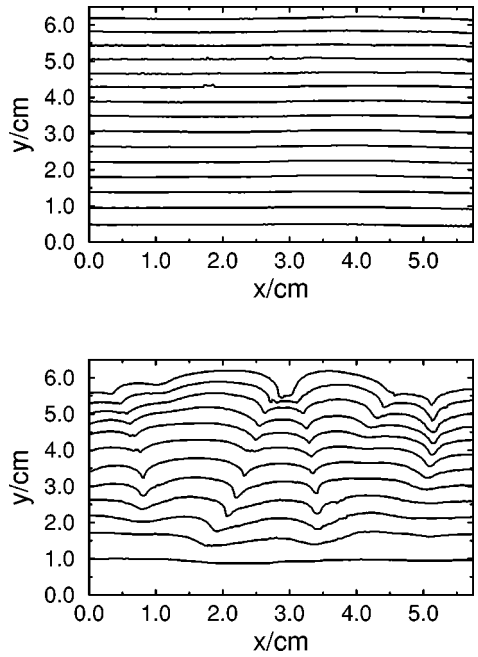

FIG. 2. Superposed front profiles showing the evolution of front structure from a planar initiation for (top) $c_M = 6.0$ mM (20% binding); (bottom) $c_M = 21.0$ mM (70% binding). The time intervals are (top) 20 min; (bottom) 120 min. Conditions and reagent concentrations are the same as in Fig. 1.

eters $\kappa = 1.0$ and $\mu = 0.0-4.2$ corresponded to the experimental conditions, while $K = 0.002$ was set using a dissociation constant typical for small carboxylic acids, and $\delta = 2$ was chosen to indicate that free hydrogen ions presumably diffuse faster than the reactant ions in the hydrogel.

IV. RESULTS AND DISCUSSION

Upon initiation, a planar front develops along the interface between the two parts of the gel which then propagates toward the reactant medium. In gels with little methacrylate content the planar front is stable, retaining its geometry as shown in Fig. 1(a). At higher methacrylate concentrations, however, the planar front loses stability, yielding a cellular structure [see Fig. 1(b)] where the cells having slightly curved leading segments are joined in sharp cusps. The evolutions of the planar and the cellular structures are compared in Fig. 2. In the latter, the inherent noise is amplified by the dominating diffusion of reactants due to the high methacrylate content, leading to the creation of cells (see bottom in Fig. 2), while in the former it decays, leaving the planar geometry stable (top of Fig. 2). The size of the cells formed are between 1 and 1.5 cm and independent of the initiation and the size of the domain. In experiments carried out in narrow strips of gels, the planar front remains stable even at high methacrylate concentrations when the width of the domain ($w = 0.5$ cm) is less then the natural size of a cell. By increasing the width of the medium, first a single cell appears ($w = 1.0$ cm), followed by the formation of a cusp separating two cells ($1.5\ \text{cm} \leqslant w \leqslant 3.0\ \text{cm}$). At even wider gels, more cells are able to fit along the front. Not only the size and location of the cells vary with time as the cusps separating them exhibit transverse motion within the front, but also their number fluctuates as a cell disappears when neighboring cusps collide or a large cell divides when a new cusp develops in the middle. This dynamic rearrangement of the cellular structure can readily be demonstrated by locating the cusps during front propagation, as shown in Fig. 3. The periodicity of this motion, however, cannot be determined experimentally in closed systems due to the long time scales related to the transverse waves.

The extent of instability can be represented with the maximum deviation from the planar symmetry, which we define as the maximum distance in the direction of propagation between the foremost segment of a cell and the hindmost cusp within a front. Since the cellular structure constantly changes, a temporal average is taken as the front propagates. The evaluation of this amplitude for fronts in gels with varying methacrylate content allows the experi-

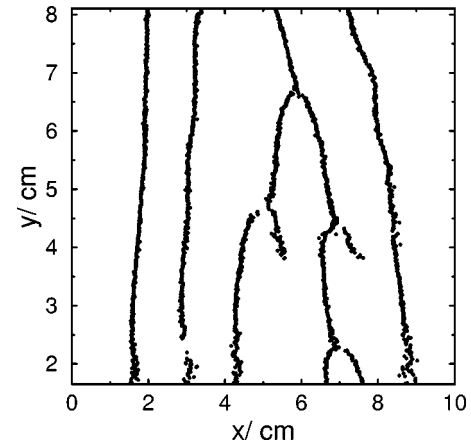

FIG. 3. The evolution of cusps—defined as local minima in the front profiles—for a front with high methacrylate content ($c_M = 21.0$ mM).

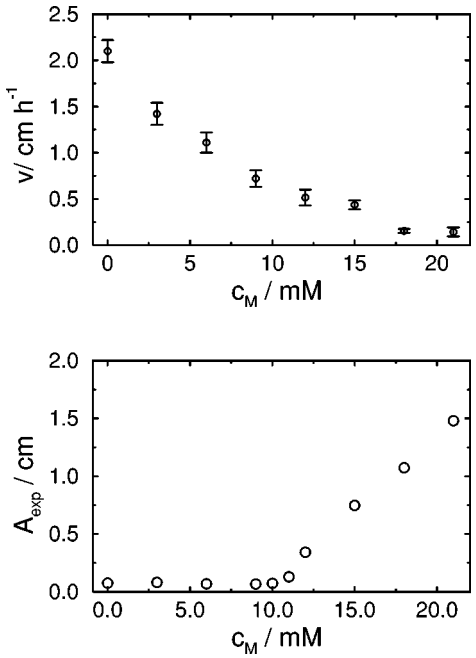

FIG. 4. The effect of methacrylate concentration on the velocity of propagation (top) and the average amplitude (bottom) of the fronts.

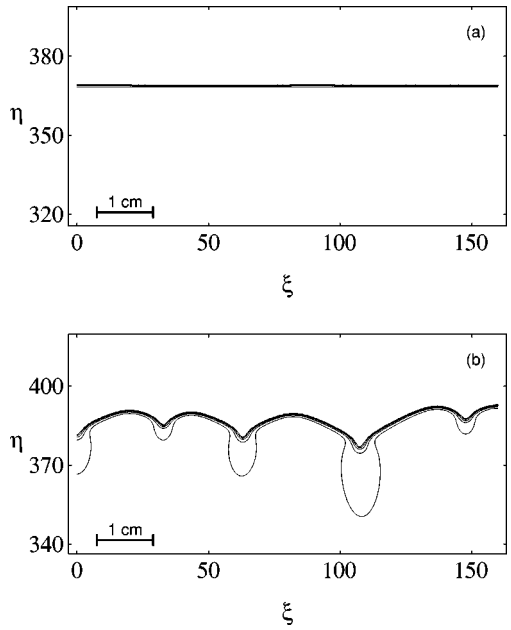

FIG. 5. Contour lines representing the calculated fronts developed from planar initiation with small random perturbation for (a) $\mu=1.2$ at $\tau=80$; (b) $\mu=4.2$ at $\tau=600$. The contour lines are drawn at (a) $\beta=0.7$, 1.4, 2.1, 2.8, 3.5; (b) $\beta=0.25$, 0.55, 0.85, 1.15, 1.45. The extent of binding for the autocatalyst corresponds to the experiments shown in Fig. 1: 20% and 70%, respectively. For the calculation of length scale, $D=2\times10^{-5}$ cm^2 s^{-1} was taken.

mental determination of the critical methacrylate concentration where the planar front loses stability. As shown in Fig. 4, with increasing methacrylate content in the hydrogel, the velocity of propagation decreases monotonously; however, the amplitude of the front is only zero within the experimental error for $c_M \leqslant (10.5\pm0.5)$ mM, indicating a stable planar front. Above this critical value a cellular front structure emerges with increasing amplitude.

In the calculations at low dimensionless methacrylate concentrations, the initial perturbation in the front decays, leaving the planar symmetry stable as shown in Fig. 5(a). At high values of μ, however, the initially imposed random noise is amplified, leading to the destabilization of the planar front, which results in the formation of cellular structures [see Fig. 5(b)] similarly to experimental observations. The calculations shown in Fig. 5 correspond to the same extent of binding for the autocatalyst hydrogen ions as in the experiments depicted in Fig. 1. The contour lines also illustrate a general feature of cellular fronts that the deviation from the planar structure is more significant toward the end of the reaction, i.e., at high values of β. The choice of congo red in the experiments has utilized this feature, since the indicator changes color in the acidic region at high extent of reaction allowing the visualization of larger amplitudes in the fronts. Comparison of Figs. 1 and 5 reveals that the simple model is able to reproduce the experimental observations. The physical size of the obtained patterns mainly depends on the actual value of the diffusion coefficients of reactants, for which we used the value generally accepted for dilute solutions $D=2\times10^{-5}$ cm^2 s^{-1}, since running the reactions in hydrogel did not affect the velocity of propagation compared to normal aqueous solutions with identical composition.

At the applied grid size, the evolution of cells resembles the experimental observations at equivalent gel widths. As the cusps exhibit transverse motion, shrinking cells disappear upon their collision (see Fig. 6) or large cells may break up, yielding a cusp in the center.

In analogy to experiments, an average amplitude is calculated for front positions—defined as the coordinate η of the maximum rate of reaction r—to determine the critical value of μ for the onset of instability. As shown in Fig. 7, planar front is stable for $\mu<\mu_{cr}=3.0\pm0.1$ with monotonously decreasing velocity of propagation. At higher μ, the cellular front structure is stable with increasing amplitude.

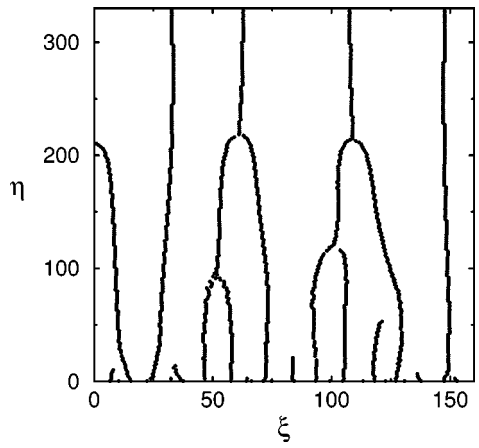

FIG. 6. Dynamic rearrangement of the cellular structure in the calculated fronts shown by the positions of the local minima in the front profile for $\mu=4.2$.

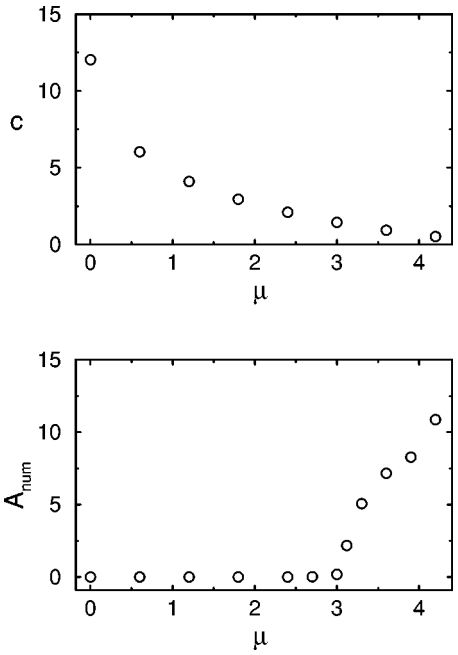

FIG. 7. The effect of dimensionless methacrylate concentration μ on the velocity of propagation (top) and on the average amplitude (bottom) of the calculated fronts. The range of μ corresponds to the experimentally spanned region of methacrylate concentration shown in Fig. 4.

Considering the experimental results shown in Fig. 4, the critical value of μ from the calculations corresponds to a slightly higher methacrylate concentration $c_M = 15.0$ mM. Further calculations have shown that μ_{cr} depends on the ratio of diffusion coefficients; at $\delta = 1$ the calculated onset of front instability corresponds to the experimentally determined critical methacrylate content, while it is shifted to higher values on increasing δ.

V. CONCLUSION

A systematic study of cellular fronts in the acid-catalyzed chlorite–tetrathionate reaction is presented. The instability of planar front symmetry arises as a result of the unequal diffusion of interacting species caused by selective binding of the autocatalyst. In the newly developed method, the application of a strong binder for the autocatalyst provides a more effective immobilization, since only a small amount of carboxylate is sufficient in contrast to former methods, where an excess amount of complexing agent with relatively weak binding capability was necessary to achieve the appropriate immobilization.[15] An increase of the methacrylate content has led to the determination of a critical concentration above which planar fronts lose stability, resulting in the formation of cellular structures with increasing amplitude in the front profiles. The simple two-variable model based on the empirical rate law has been shown to reproduce the experimental observations without the use of adjustable parameters. We anticipate that cellular structures may be general features of reaction–diffusion fronts, as there are several acid-catalyzed reactions producing propagating fronts in spatially distributed systems,[22] where the component species can be spatially decoupled by running the reactions in gelled medium selectively binding the autocatalyst hydrogen ions.

ACKNOWLEDGMENTS

We thank István Lagzi for carrying out some preliminary experiments. This work was supported by the Hungarian Science Foundation, OTKA (Grant Nos. F022037 and D24071). D.H. thanks the Foundation for Hungarian Higher Education and Research for a Magyary Zoltán Fellowship.

[1] A. M. Turing, Philos. Trans. R. Soc. London, Ser. B **237**, 37 (1952).
[2] G. Nicolis and I. Prigogine, *Self-Organization in Nonequilibrium Chemical Systems* (Wiley, New York, 1977).
[3] H. Haken, *Synergetics, An Introduction* (Springer-Verlag, Berlin, 1977).
[4] J. D. Murray, *Mathematical Biology* (Springer-Verlag, Berlin, 1989).
[5] V. Dufiet and J. Boissonade, J. Chem. Phys. **98**, 664 (1992).
[6] V. Castets, E. Dulos, J. Boissonade, and P. De Kepper, Phys. Rev. Lett. **64**, 2953 (1990).
[7] Q. Ouyang and H. L. Swinney, Nature (London) **352**, 610 (1991).
[8] I. Lengyel, S. Kádár, and I. R. Epstein, Science **259**, 493 (1993).
[9] K. J. Lee, W. D. McCormick, Q. Ouyang, and H. L. Swinney, Science **261**, 192 (1993).
[10] K. J. Lee, W. D. McCormick, J. E. Pearson, and H. L. Swinney, Nature (London) **369**, 215 (1994).
[11] K. J. Lee and H. L. Swinney, Phys. Rev. E **51**, 1899 (1995).
[12] Y. Kuramoto and T. Tsuzuki, Prog. Theor. Phys. **55**, 356 (1976).
[13] Y. Kuramoto, in *Dynamics of Synergetic Systems*, edited by H. Haken (Springer, Berlin, 1980), pp. 134–146.
[14] D. Horváth, V. Petrov, S. K. Scott, and K. Showalter, J. Chem. Phys. **98**, 6332 (1993).
[15] D. Horváth and K. Showalter, J. Chem. Phys. **102**, 2471 (1995).
[16] Á. Tóth, I. Lagzi, and D. Horváth, J. Phys. Chem. **100**, 14837 (1996).
[17] I. Lengyel and I. R. Epstein, Proc. Natl. Acad. Sci. USA **89**, 3977 (1992).
[18] G. H. Markstein, J. Aeronaut. Sci. **3**, 18 (1951).
[19] G. I. Sivashinsky, Combust. Sci. Technol. **15**, 137 (1977).
[20] I. Nagypál and I. R. Epstein, J. Phys. Chem. **90**, 6285 (1986).
[21] Á. Tóth, D. Horváth, and A. Siska, J. Chem. Soc. Faraday Trans. **93**, 73 (1997).
[22] L. Szirovicza, I. Nagypál, and E. Boga, J. Am. Chem. Soc. **111**, 2842 (1989).